C. R. Mecanique 340 (2012) 661–667

Contents lists available at SciVerse ScienceDirect

Comptes Rendus Mecanique

www.sciencedirect.com

A piezoelectric screw dislocation near an elliptical inhomogeneity containing a confocal rigid line

C.Z. Jiang [a,b,c,*], Y.X. Zhao [a,b], Y.W. Liu [a,b]

[a] State Key Laboratory of Advanced Design and Manufacturing for Vehicle Body, Hunan University, Changsha 410082, PR China
[b] College of Mechanical and Vehicle Engineering, Hunan University, Changsha 410082, PR China
[c] Department of Physics and Electronic Information Engineering, Xiangnan University, Chenzhou 423000, PR China

ARTICLE INFO

Article history:
Received 23 May 2012
Accepted after revision 10 July 2012
Available online 1 September 2012

Keywords:
Material engineering
Piezoelectric screw dislocation
Elliptical inhomogeneity
Rigid line
Complex variable method

ABSTRACT

The interaction between a piezoelectric screw dislocation and an elliptical inhomogeneity in piezoelectric composite material which contains an electrically conductive confocal rigid line is studied, especially analyzing the shielding effect of a piezoelectric screw dislocation near an elliptical inhomogeneity. By applying the complex variable method, the analytical solution to the elastic field and the electric field, the field intensity factors at the tip of the rigid line are derived. The image force acting on the piezoelectric screw dislocation is calculated by using the generalized Peach–Koehler formula. Accordingly, the location and the orientation of the dislocation, the material properties upon the shielding or anti-shielding effect on the stress intensity factors, as well as the effects of the rigid line and the electroelastic properties of the piezoelectric materials on the image force are discussed.

1. Introduction

Piezoelectric materials are widely used in modern technology such as sensors, micropositioner, electro-mechanical actuator and high power sonar transducers as a result of the intrinsic coupling behavior [1–5]. However, the presence of various defects, such as dislocations, cracks and inclusions, can greatly influence their characteristics and coupling behavior. So it is important to investigate the electro-elastic fields as a result of the presence of defects and inhomogeneities in these quasi-brittle solids. The intensity of the electro-elastic fields near the tip of the crack or anti-crack (rigid line) in piezoelectric materials could be characterized by a factor depending on geometric shapes, loading conditions and the material properties, etc. Above the factor are known as the field intensity factors, which may include the stress intensity factor (SIF) of the elastic fields and the electric displacement intensity factor of the electric fields. The field intensity factors can be used to be an indicator to if the crack will propagate or not. When the field intensity factors are greater than the critical field intensity factors, the crack will propagate. Here the critical field intensity factors are determined by the experiment, and relate to many parameters, such as temperature, plate thickness, strain velocity, etc. There are many articles [6–12] in which the electro-elastic coupling behavior of the inhomogeneity and dislocation in piezoelectric materials has been deeply researched in recent years. The schistose rigid inclusion can be formed inside reinforcement due to chemical composition segregation during the crystallizing process in the piezoelectric materials. Fang and Li [13] considered the problem for the electro-elastic interaction between a piezoelectric moving dislocation and interfacial collinear rigid lines under combined longitudinal shear and in-plane electric field. Then Fang [14] investigated the interaction between a screw dislocation and an elliptical inclusion with interfacial rigid lines in piezoelectric solids. Wu and Du [15] discussed the elastic field and electric field of a rigid line in a confocal elliptic piezoelectric inhomogeneity embedded in an infinite piezoelectric medium

* Corresponding author at: Department of Physics and Electronic Information Engineering, Xiangnan University, Chenzhou 423000, PR China.
E-mail address: jiangchunzhi@126.com (C.Z. Jiang).

1631-0721/$ – see front matter
http://dx.doi.org/10.1016/j.crme.2012.07.002

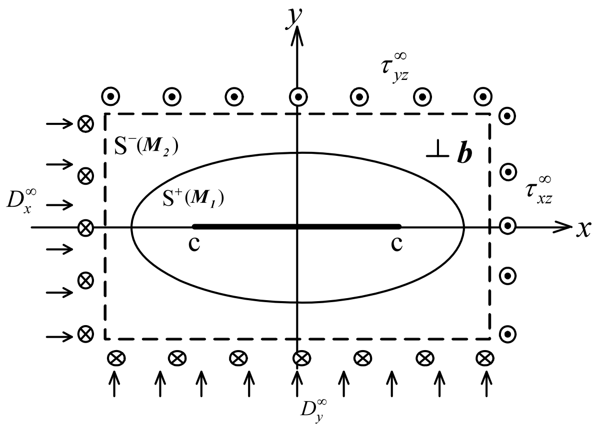

Fig. 1. The model in physical plane.

under the remote anti-plane shear and in-plane electric field, and analyzed the characteristics of the elastic field and electric field singularities at the rigid line tip. However, the interaction of a piezoelectric screw dislocation with a rigid line in a confocal elliptic inhomogeneity has not been studied due to the complexity of the calculation. In the current paper, the electro-elastic coupling interaction between a piezoelectric screw dislocation and an elliptical inhomogeneity, and the shielding effect of a piezoelectric screw dislocation on the rigid line are studied by using the complex variable method of singularity principal analysis, conformal mapping, analytic continuation and Cauchy singular integral.

2. Statement of the problem and solution

Consider an infinite piezoelectric matrix containing an elliptical cylindrical inhomogeneity with an electrically conductive confocal rigid line which is infinitely long in the z-direction and free of force, under in-plane electrical loads. Both the matrix and the inhomogeneity are assumed to be transversely isotropic with an isotropic xoy-plane. A piezoelectric screw dislocation $\boldsymbol{b} = \{b_z\ b_\varphi\}^T$ is located at arbitrary point z_0 in the matrix.

For the present problem, out-of-plane displacement and in-plane electric field need to be considered, so that there are only non-trivial displacement w, strains γ_{xz} and γ_{yz}, stresses τ_{xz} and τ_{yz}, electrical field components E_x and E_y, electric potential φ and electric displacement components D_x and D_y in the Cartesian coordinates. All components are only functions of x and y. Introducing the vector of generalized displacement $\boldsymbol{U} = \left\{\begin{smallmatrix} w \\ \varphi \end{smallmatrix}\right\}$, the generalized strains $\boldsymbol{Y}_x = \left\{\begin{smallmatrix} \gamma_{xz} \\ -E_x \end{smallmatrix}\right\}$, $\boldsymbol{Y}_y = \left\{\begin{smallmatrix} \gamma_{yz} \\ -E_y \end{smallmatrix}\right\}$ and generalized stresses $\boldsymbol{\Sigma}_x = \left\{\begin{smallmatrix} \tau_{xz} \\ D_x \end{smallmatrix}\right\}$ and $\boldsymbol{\Sigma}_y = \left\{\begin{smallmatrix} \tau_{yz} \\ D_y \end{smallmatrix}\right\}$ can be written with an analytical function vector $\boldsymbol{f}(z) = \{f_w(z)\ f_\varphi(z)\}^T$, where $z = x + iy$ is the complex variable.

$$\boldsymbol{U} = \mathrm{Re}\big[\boldsymbol{f}(z)\big] \qquad \boldsymbol{Y}_x - i\boldsymbol{Y}_y = \boldsymbol{f}'(z) \qquad \boldsymbol{\Sigma}_x - i\boldsymbol{\Sigma}_y = \boldsymbol{M}\boldsymbol{f}'(z) \tag{1}$$

where $\boldsymbol{M} = \left[\begin{smallmatrix} C_{44} & e_{15} \\ e_{15} & -d_{11} \end{smallmatrix}\right]$, C_{44}, e_{15} and d_{11} are the elastic, piezoelectric and dielectric constants, respectively.

In order to facilitate the analysis, we introduce the following function vector

$$\boldsymbol{T} = \int_A^B (\boldsymbol{\Sigma}_x\,\mathrm{d}y - \boldsymbol{\Sigma}_y\,\mathrm{d}x) = \boldsymbol{M}\mathrm{Im}\big[\boldsymbol{f}(z)\big]_A^B \tag{2}$$

where $[\,]_A^B$ represents the change in the bracketed function vector from point A to point B along any arc AB (not passing through interfaces of dissimilar phase).

Introducing the following mapping function [16]

$$z = \omega(\zeta) = \frac{c}{2}\left(R\zeta + \frac{1}{R\zeta}\right) \quad R\zeta = \frac{z}{c}\left[1 + \sqrt{1 - \left(\frac{c}{z}\right)^2}\,\right] \tag{3}$$

where $\zeta = \xi + i\eta$, $c = \sqrt{a^2 - b^2}$, $R = \sqrt{\frac{a+b}{a-b}}$, $\zeta = re^{i\theta}$. Using the mapping function, the elliptical curve and the rigid line in the z-plane ($z = re^{i\theta}$) are mapped onto the concentric circles in the ζ-plane ($\zeta = \varsigma e^{i\varphi}$) with radius 1, $\frac{1}{R}$, respectively, see Fig. 1 and Fig. 2.

With the mapping function (3), Eqs. (1) and (2) can be rewritten in the ζ-plane.

The hypothesis of the perfect bonding between the medium S^+ and the medium S^- implies that

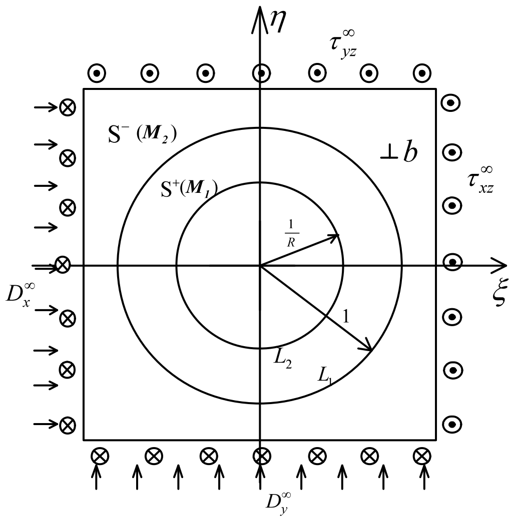

Fig. 2. The model in transformed plane.

$$\boldsymbol{U}_1^+(t) = \boldsymbol{U}_2^-(t) \qquad \boldsymbol{T}_1^+(t) = \boldsymbol{T}_2^-(t) \quad \text{along the interface } |t| = 1 \tag{4}$$

where the subscripts 1 and 2 represent the regions inhomogeneity S^+ and matrix S^-. The superscripts $+$ and $-$ denote the boundary values of the physical quantity as z approaches the interface from S^+ and S^-, respectively.

According to the Schwarz symmetry principle, the following new analytical function vectors are introduced in the corresponding region

$$\boldsymbol{f}_{1*}(\zeta) = -\bar{\boldsymbol{f}}_1\left(\frac{1}{\zeta}\right) \quad 1 < |\zeta| < R \tag{5}$$

$$\boldsymbol{f}_{2*}(\zeta) = -\bar{\boldsymbol{f}}_2\left(\frac{1}{\zeta}\right) \quad |\zeta| < 1 \tag{6}$$

Then the boundary conditions express as

$$\left[\boldsymbol{f}_1(\zeta) + \boldsymbol{f}_{2*}(\zeta)\right]^+ = \left[\boldsymbol{f}_2(t) + \boldsymbol{f}_{1*}(t)\right]^- \quad |t| = 1 \tag{7}$$

$$\left[\boldsymbol{M}_1\boldsymbol{f}_1(t) - \boldsymbol{M}_2\boldsymbol{f}_{2*}(t)\right]^+ = \left[\boldsymbol{M}_2\boldsymbol{f}_2(t) - \boldsymbol{M}_1\boldsymbol{f}_{1*}(t)\right]^- \quad |t| = 1 \tag{8}$$

The generalized analytical function vector in the matrix as

$$\boldsymbol{f}_2(z) = \boldsymbol{B}\ln(z - z_0) + \boldsymbol{f}_{20}(z) \quad z \in S^- \tag{9}$$

where $\boldsymbol{B} = \frac{\boldsymbol{b}}{2\pi i}$, $\boldsymbol{f}_{20}(z)$ is holomorphic in the region S^-.

Transforming into ζ-plane, we obtain

$$\boldsymbol{f}_2(\zeta) = \boldsymbol{B}\ln(\zeta - \zeta_0) + \boldsymbol{f}_{20}(\zeta) \quad |\zeta| > 1 \tag{10}$$

where $\boldsymbol{f}_{20}(\zeta)$ is holomorphic in the region $|\zeta| > 1$.

$\boldsymbol{f}_1(\zeta)$ can be expanded into a Laurent series in the annular region

$$\boldsymbol{f}_1(\zeta) = \sum_{k=0}^{\infty}\boldsymbol{a}_k\zeta^{k+1} + \sum_{k=0}^{\infty}\boldsymbol{b}_k\zeta^{-(k+1)} \quad \boldsymbol{a}_k \text{ and } \boldsymbol{b}_k \text{ are complex constant vectors, } \frac{1}{R} < |\zeta| < 1 \tag{11}$$

The boundary value problems of Eqs. (7) and (8) can be solved by using the Cauchy integrals, and then we can obtain the generalized analytical function vectors.

$$\boldsymbol{f}_1(\zeta) = -2\sum_{k=0}^{\infty}\frac{\boldsymbol{\Lambda}^{-1}\boldsymbol{M}_2\boldsymbol{B}}{(k+1)}\cdot\left[\left(\frac{R^2\zeta}{\zeta_0}\right)^{k+1} + \left(\frac{1}{\overline{\zeta_0}\zeta}\right)^{k+1}\right] \tag{12}$$

$$\boldsymbol{f}_2(\zeta) = \boldsymbol{B}\ln(\zeta - \zeta_0) - \sum_{k=0}^{\infty}\frac{\boldsymbol{B}}{k+1}(\overline{\zeta_0}\zeta)^{-k-1} + 2\sum_{k=0}^{\infty}\frac{\boldsymbol{\Lambda}^{-1}\boldsymbol{M}_2\boldsymbol{B}}{(k+1)}\cdot\left[R^{2k+2} - 1\right](\overline{\zeta_0}\zeta)^{-k-1} \tag{13}$$

where $\boldsymbol{\Lambda} = [(\boldsymbol{M}_1 + \boldsymbol{M}_2)R^{2k+2} + (\boldsymbol{M}_1 - \boldsymbol{M}_2)]$.

If $\boldsymbol{M}_1 = \boldsymbol{M}_2$, the solution on the interaction between a piezoelectric screw dislocation and a finite-length rigid line in homogeneous piezoelectric material can be calculated

$$\boldsymbol{f}_1(\zeta) = -\sum_{k=0}^{\infty} \frac{\boldsymbol{B}}{(k+1)\mathrm{R}^{2k+2}} \cdot \left[\left(\frac{R^2 \zeta}{\zeta_0} \right)^{k+1} + \left(\frac{1}{\overline{\zeta_0} \zeta} \right)^{k+1} \right] \tag{14}$$

$$\boldsymbol{f}_2(\zeta) = \boldsymbol{B} \ln(\zeta - \zeta_0) - \sum_{k=0}^{\infty} \frac{\boldsymbol{B}}{(k+1)R^{2k+2}} (\overline{\zeta_0} \zeta)^{-k-1} \tag{15}$$

If we take $\boldsymbol{M} = \left[\begin{smallmatrix} c_{44} & 0 \\ 0 & 0 \end{smallmatrix}\right]$, $b \to a$, then $c \to 0$ and $R \to \infty$, the solutions are reduced to the interaction between a screw dislocation and a circular inhomogeneity in elastic material,

$$\boldsymbol{f}_1(\zeta) = -2 \sum_{k=0}^{\infty} \frac{[\boldsymbol{M}_1 + \boldsymbol{M}_2]^{-1} \boldsymbol{M}_2 \boldsymbol{B}}{k+1} \cdot \left(\frac{\zeta}{\zeta_0} \right)^{k+1} \tag{16}$$

$$\boldsymbol{f}_2(\zeta) = \boldsymbol{B} \ln(\zeta - \zeta_0) - \sum_{k=0}^{\infty} \frac{\boldsymbol{B}}{k+1} (\overline{\zeta_0} \zeta)^{-k-1} + 2 \sum_{k=0}^{\infty} \frac{[\boldsymbol{M}_1 + \boldsymbol{M}_2]^{-\mathbf{1}} \boldsymbol{M}_2 \boldsymbol{B}}{k+1} (\overline{\zeta_0} \zeta)^{-k-1} \tag{17}$$

which are in agreement with the results in [17].

3. Field intensity factors

The field intensity factors are important parameters of piezoelectric composite material. According to [18], the field intensity factors at the right tip of the rigid line can be calculated as

$$\boldsymbol{K} = \begin{bmatrix} k_3 \\ k_D \end{bmatrix} = \sqrt{2\pi} \lim_{\zeta \to 1/R} \sqrt{\omega(\zeta) - \omega(1/R)} \, [\, \tau_{yz} \quad D_y \,]^T = \frac{1}{iR\sqrt{\pi c}} \sum_{k=0}^{\infty} \boldsymbol{M}_1 \boldsymbol{\Lambda}^{-1} \boldsymbol{M}_2 \boldsymbol{b} \cdot \left[\frac{R^{k+2}}{\overline{\zeta_0}^{k+1}} - \frac{R^{k+2}}{\zeta_0^{k+1}} \right] \tag{18}$$

where k_3 is the stress intensity factor, k_D is the electric displacement intensity factor.

4. Perturbation stress and image force on the dislocation

One of the major interests in discussing the interaction problem of the piezoelectric dislocation with the inhomogeneity is the image forces on the piezoelectric screw dislocation. According to the generalized Peach–Koehler formula [19], the image forces can be written as

$$F_x - iF_y = \left[\frac{1}{2\pi} \sum_{k=0}^{\infty} \boldsymbol{b}^T \boldsymbol{M}_2 \boldsymbol{b} \overline{\zeta_0}^{-k-1} \zeta_0^{-k-2} - \frac{1}{\pi} \sum_{k=0}^{\infty} \boldsymbol{b}^T \boldsymbol{M}_2 \boldsymbol{\Lambda}^{-1} \boldsymbol{M}_2 \boldsymbol{b} \left(R^{2K+2} - 1 \right) \overline{\zeta_0}^{-k-1} \zeta_0^{-k-2} \right] \cdot \frac{2R\zeta_0^2}{cR^2 \zeta_0^2 - c} \tag{19}$$

5. Numerical examples and discussion

It is shown in Eq. (18), that the field intensity factors are directly proportional to $\boldsymbol{b}$ and relevant to the location of the dislocation $\zeta_0 = r_0 e^{i\theta}$ when the size of the inhomogeneity and material constants are certain. The stress intensity factor and the electric displacement intensity factor are all equal to zero as the dislocation lies on x-axis.

As a practical example, we assume that the piezoelectric screw dislocation is $\boldsymbol{b} = \{1.0 \times 10^{-9} \text{ m } 0\}^T$, the piezoelectric matrix is PZT-5H with the electroelastic properties: $C_{44}^{(2)} = 2.56 \times 10^{10}$ N/m^2, $e_{15}^{(2)} = 12.7$ C/m^2, $d_{11}^{(2)} = 0.646 \times 10^{-8}$ C/V m. The inhomogeneity is another piezoelectric material. Let us introduce the shear modulus ratio $u = C_{44}^{(2)}/C_{44}^{(1)}$, piezoelectric coefficients ratio $v = e_{15}^{(2)}/e_{15}^{(1)}$ and dielectric constants ratio $d_{11}^{(2)}/d_{11}^{(1)} = 1$.

The normalized stress intensity factor is $k_{30} = \frac{\sqrt{\pi c}}{C_{44}^{(2)} b_z} k_3$. The variation of k_{30} with respect to θ with different values of u for piezoelectric material and elastic material when $r_0 = 1.5$ are depicted in Fig. 1 and Fig. 2, respectively. Fig. 3 shows k_{30} versus θ with different values of v, and Fig. 4 shows k_{30} versus r with different values of u when $\theta = \pi/3$.

It can be found from Figs. 3–6, when a positive screw dislocation is located in the upper half-plane, the stress intensity factor will be positive (anti-shielding effect); while in the lower half-plane, the stress intensity factor will be negative (shielding effect). The absolute value of k_{30} increases with the decrement of u, namely, the shielding or anti-shielding effect on the stress intensity factor of the rigid line increases with the decrement of the shear modulus ratio. A comparison of Fig. 3 with Fig. 4 indicates that the piezoelectric properties can enhance the shielding effect of the screw dislocation. It is also found that the shielding or anti-shielding effect will weaken gradually with the dislocation move away from the

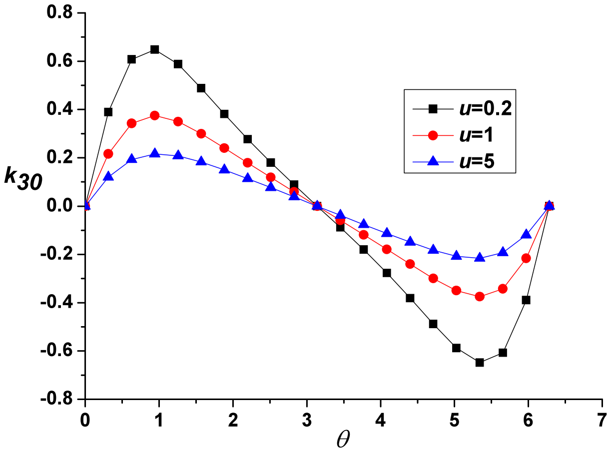

Fig. 3. k_{30} versus θ with different u and $v = 1$.

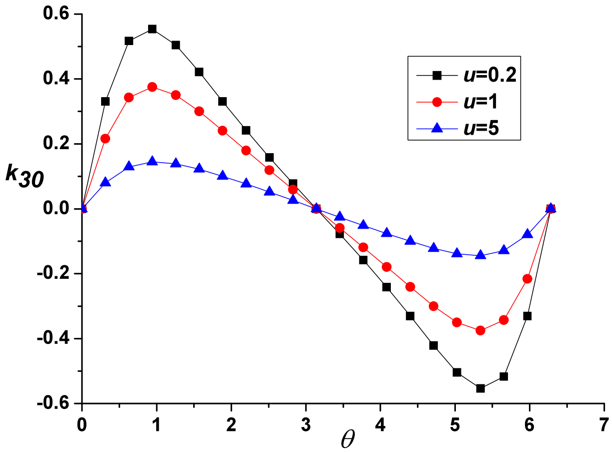

Fig. 4. k_{30} versus θ with different u for elastic material.

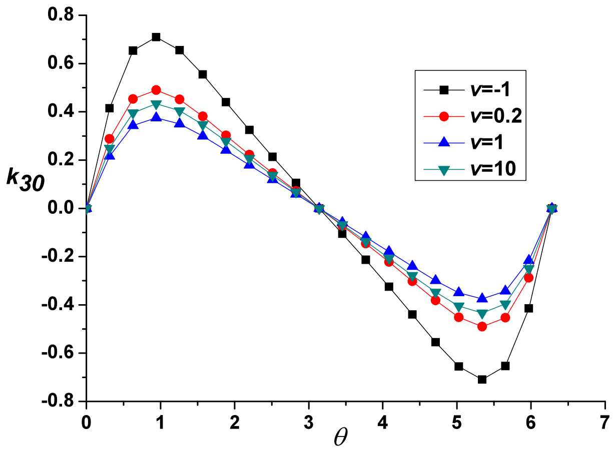

Fig. 5. k_{30} versus θ with different v and $u = 1$.

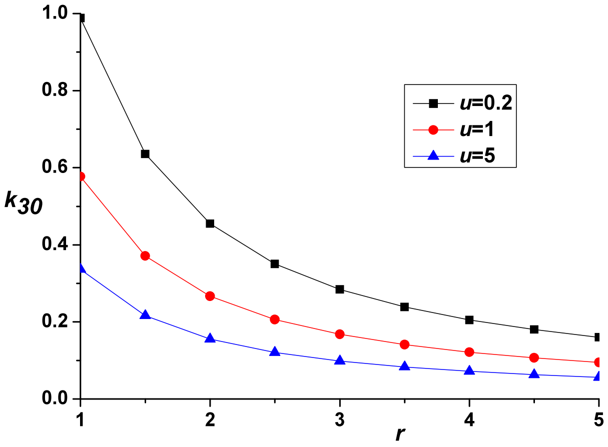

Fig. 6. k_{30} versus r with different u and $v = 1$.

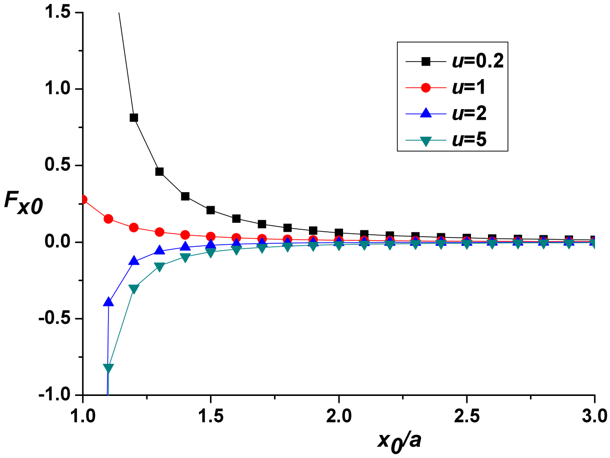

Fig. 7. F_{x0} versus x_0/a with different u, $v = 1$.

interface of the inhomogeneity, and the smaller the shear modulus ratio, the greater the rate of change of the shielding or anti-shielding effect.

The influence of the different parameters to the image force can be analyzed by using Eq. (19).

If the dislocation lies on the x-axis ($z_0 = x_0$), let us define $F_{x0} = 2\pi F_x / C_{44}^{(2} b_z^2$. Fig. 7 shows F_{x0} versus x_0/a with different u as $v = 1$. It can be found that the absolute value of F_{x0} may be increased acutely from zero when the screw dislocation approaches the interface of the inclusion. The image force is always positive as $u \leqslant 1$, for which the rigid line and the stiff inhomogeneity repel the screw dislocation. There exists an unstable equilibrium position of the screw dislocation in the matrix and the image force equals zero at that point for the case as $u > 1$.

The variation of F_{x0} with respect to u is given in Fig. 8 with different x_0/a. We observe that the unstable equilibrium position of the screw dislocation only appear near the elliptical interface. The influence of the shear modulus ratio on the image force will decrease acutely as the distance between the screw dislocation and the elliptical interface increases.

6. Conclusions

The problem of the electroelastic interaction between a piezoelectric screw dislocation and an elliptical inclusion containing a rigid line under in-plane electrical loads is dealt with by using of an efficient complex variable method. The explicit series solutions for the complex potentials of the matrix and the inclusion, as well as the field intensity factors at the tip of the rigid line are calculated. The generalized Peach–Koehler force acting on the screw dislocation is also given. The results show that the electroelastic properties of the material, the location and the orientation of the dislocation have large influence of the shielding or anti-shielding effect on the stress intensity factors of the rigid line. The shielding effect of the screw dislocation in piezoelectric composite material is better than that in corresponding elastic material. The effect of the rigid line on the equilibrium position of the dislocation near an elliptical inclusion is significant. An unstable equilibrium position of the screw dislocation in the matrix can exist when the dislocation near the soft elliptical inclusion.

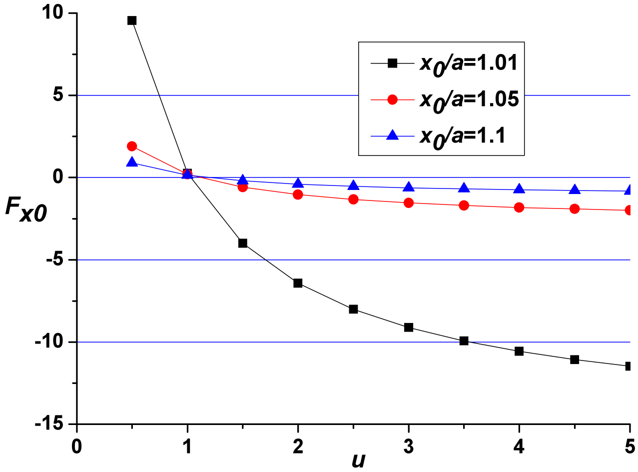

Fig. 8. F_{x0} versus u with different x_0/a, $v = 1$.

Acknowledgements

The authors gratefully acknowledge research support from the Science Fund of State Key Laboratory of Advanced Design and Manufacturing for Vehicle Body (No. 60870005), the NNSFC (11172094 and 11172095) and the NCET-11-0122. The work was also supported by the Fundamental Research Funds for the Central Universities, Hunan University.

References

[1] F. dell'Isola, M. Porfiri, S. Vidoli, Piezo-electromechanical (PEM) structures: passive vibration control using distributed piezoelectric transducers, C. R. Mecanique 331 (2003) 69–76.
[2] C. Falconi, G. Mantini, A. D'Amico, Z.L. Wang, Studying piezoelectric nanowires and nanowalls for energy harvesting, Sens. Actuators B 139 (2009) 511–519.
[3] A. Mahieddine, J. Pouget, M. Ouali, Modeling and analysis of delaminated beams with integrated piezoelectric actuators, C. R. Mecanique 338 (2010) 283–289.
[4] Y.D. Li, K.Y. Lee, N. Zhang, A generalized hypergeometric function method for axisymmetric vibration analysis of a piezoelectric actuator, Eur. J. Mech. A Solids 31 (2012) 110–116.
[5] T. Weller, C. Licht, Asymptotic modeling of piezoelectric plates with electric field gradient, C. R. Mecanique 340 (6) (2012) 405–410.
[6] Z. Huang, Z.B. Kuang, Dislocation inside a piezoelectric media with an elliptical inhomogeneity, Int. J. Solids Struct. 38 (2001) 8459–8480.
[7] B.J. Chen, Z.M. Xiao, K.M. Liew, A screw dislocation in a piezoelectric bi-material wedge, Int. J. Eng. Sci. 40 (2002) 1665–1685.
[8] B.J. Chen, Z.M. Xiao, K.M. Liew, A piezoelectric screw dislocation near a wedge-shaped bi-material interface, Int. J. Solids Struct. 40 (2003) 2041–2056.
[9] Y.W. Liu, Q.H. Fang, C.P. Jiang, A piezoelectric screw dislocation interacting with an interphase layer between a circular inclusion and the matrix, Int. J. Solids Struct. 41 (2004) 3255–3274.
[10] Y.W. Liu, Q.H. Fang, Electroelastic interaction between a piezoelectric screw dislocation and a circular inhomogeneity with interfacial cracks, Appl. Math. Mech. 12 (2004) 1325–1332.
[11] X. Wang, E. Pan, A moving screw dislocation interacting with an imperfect piezoelectric bimaterial interface, Phys. Status Solidi B 244 (2007) 1940–1956.
[12] X. Wang, E. Pan, Interaction between a screw dislocation and a viscoelastic piezoelectric bimaterial interface, Int. J. Solids Struct. 45 (2008) 245–257.
[13] Q.H. Fang, B. Li, Y.W. Liu, Electro-elastic interaction between a moving screw dislocation and collinear interfacial rigid lines, Mater. Sci. Eng. A 430 (2006) 46–58.
[14] Q.H. Fang, Y.W. Liu, P.H. Wen, A piezoelectric dislocation interacting with an elliptical inclusion containing electrically conductive interfacial rigid lines, Int. J. Mech. Sci. 50 (2008) 683–693.
[15] L.Z. Wu, S.Y. Du, A rigid line in a confocal elliptic piezoelectric inhomogeneity embedded in an infinite piezoelectric medium, Int. J. Solids Struct. 37 (2000) 1453–1469.
[16] N.L. Muskhelishvili, Some Basic Problems of Mathematical Theory of Elasticity, Noordhoff, Leyden, 1975.
[17] E. Smith, The interaction between dislocations and inhomogeneities I, Int. J. Eng. Sci. 6 (1968) 129–143.
[18] L.Z. Wu, A crack in a confocal elliptic piezoelectric inhomogeneity embedded in an infinite piezoelectric medium, Int. J. Fract. 104 (2000) 1–14.
[19] Y.E. Pak, Force on a piezoelectric screw dislocation, J. Appl. Mech. 57 (1990) 863–869.